Hindawi Publishing Corporation
International Journal of Photoenergy
Volume 2015, Article ID 795138, 10 pages
http://dx.doi.org/10.1155/2015/795138

Research Article

A Combined Effect of Plasmon Energy Transfer and Recombination Barrier in a Novel TiO_2/MgO/Ag Working Electrode for Dye-Sensitized Solar Cells

Chanu Photiphitak,[1] Pattana Rakkwamsuk,[2] Pennapa Muthitamongkol,[3] and Chanchana Thanachayanont[3]

[1]*Faculty of Science and Technology, Suan Dusit University, 295 Nakhon Ratchasima Road, Dusit, Bangkok 10300, Thailand*
[2]*School of Energy, Environment and Materials, Division of Materials Technology, King Mongkut's University of Technology Thonburi, 126 Pracha Uthit Road, Bangmod, Toongkru, Bangkok 10140, Thailand*
[3]*National Metal and Material Technology Center, 114, Thailand Science Park, Phaholyothin Road, Klong 1, Klong Luang, Pathumthani 12120, Thailand*

Correspondence should be addressed to Chanchana Thanachayanont; chanchm@mtec.or.th

Received 15 June 2015; Revised 9 August 2015; Accepted 13 August 2015

Academic Editor: Leonardo Palmisano

Novel TiO_2/MgO/Ag composite electrodes were applied as working electrodes of dye-sensitized solar cells (DSSCs). The TiO_2/MgO/Ag composite films were prepared by dip coating method for MgO thin films and photoreduction method for Ag nanoparticles. The MgO film thicknesses and the Ag nanoparticle sizes were in ranges of 0.08–0.46 nm and 4.4–38.6 nm, respectively. The TiO_2/MgO/Ag composite films were characterized by X-ray diffraction, scanning electron microscopy, and transmission electron microscopy. The TiO_2/MgO/Ag composite electrodes were sensitized by immersing in a 0.3 mM of N719 dye solution and fabricated for conventional DSSCs. *J-V* characteristics of the TiO_2/MgO/Ag DSSCs showed that the MgO film thickness of 0.1 nm and the Ag nanoparticle size of 4.4 nm resulted in maximum short circuit current density and efficiency of 8.6 mA/cm^2 and 5.2%, respectively. Electrochemical Impedance Spectroscopy showed that such values of short circuit current density and efficiency were optimal values obtained from plasmon energy transfer by 4.4 nm Ag nanoparticles and recombination barrier by the ultrathin MgO film.

1. Introduction

For more than 20 years, the first dye-sensitized solar cell (DSSC) has been published by O'Regan and Grätzel [1]. The DSSCs have been extensively studied because of their high performance, simple fabrication processes, low-cost materials, and manufacturing processes. The DSSCs consist of transparent conducting oxide (TCO) coated glass, TiO_2 photoelectrode, Ru complex photosensitizer such as N719 dye molecules, redox electrolyte such as I^-/I^{3-} (iodide/triiodide), and Pt counter electrode [2]. High performance dye-sensitized solar cells require the nanocrystalline TiO_2 electrode to have a large surface area, high crystallinity without cracks, and good electrical contact with the conducting glass substrate so that a high amount of dye molecules can be adsorbed and the electrons can be quickly transferred [3]. However, a problem of the DSSC is the low energy conversion efficiency when compared with silicon solar cells. Main reasons are charge recombination loss arising at the semiconductor/dye/electrolyte interface and low dye absorption towards the infrared region.

Recombination with the dye cations and the electrolyte species (I^{3-}) can drastically affect the open circuit voltage (V_{OC}). Improving the efficiency of DSSCs can be achieved by coating a thin film of oxide layers on the TiO_2 electrode such as MgO, ZnO, Al_2O_3, Nb_2O_5, $CaCO_3$, and $SrTiO_3$ [3, 7, 8]. The oxide film has a wide band gap that delays the electrons back transfer to the electrolyte and minimizes

charge recombination. In addition, the coating layer can increase the dye adsorption on the porous electrode and, hence, increase the photocurrent [3].

In addition, the surface plasmon resonance induced by silver (Ag) nanoparticles leads to an increase in absorption coefficient of dye in dye-sensitized solar cells (DSCs) [9–14]. The effect has been theoretically described as an increase of local electromagnetic field nearby metal surfaces which is found when wavelengths of irradiation sources are correlated with the optical absorption of the surface plasmon resonance [15–19]. The modification of the surfaces for an enhancement of optical absorption, hence, provides a good method to improve efficiency of an optoelectronic device involving photon absorption [20].

This research will improve the working electrode of the DSSCs by using both concepts of decreasing of recombination process between the electron on conduction band of TiO_2 and triiodide ion in electrolyte (I_3^-) by MgO thin film [6] and increasing of light absorption coefficient of dye molecules by silver nanoparticles [4, 5]. These are known as effects of recombination barrier and plasmon energy transfer, respectively. Therefore, the TiO_2/MgO/Ag composite film was demonstrated to be an efficient working electrode for DSSCs.

2. Materials and Methods

2.1. The Preparation of Mesoporous TiO_2 Electrodes. The TiO_2 electrodes were screen-printed from a TiO_2 paste (Dyesol) 3 times on a fluorine-doped-tin-oxide (FTO) glass substrate ($2 \times 3\,cm^2$ in size). A 200-mesh was used to obtain a TiO_2 layer with area of $0.5 \times 1.2\,cm^2$ and a thickness of approximately 13.8 μm. In order to avoid contamination on the fresh film, screen printing was performed in a clean-room environment. After drying at 55°C for 30 minutes, the electrodes were sintered at 450°C for 30 minutes and then cooled down to room temperature. The electrodes were immersed in a 3×10^{-4} M of N719 dye solution, namely, *cis*-diisothiocyanato-bis(2,2-bipyridyl-4,4-dicarboxylato)ruthenium(II) bis(tetrabutylammonium) in absolute ethanol for 24 hours. The excess dye was removed from the electrode by rinsing in ethanol.

2.2. The Preparation of Mesoporous TiO_2/MgO/Ag Composite Films. The TiO_2 film was prepared by screen printing with 3 layers and calcined at 450°C for 30 minutes. Then the TiO_2 film was dipped in a magnesium acetate solution with concentrations of 1×10^{-4}, 1×10^{-3}, and 1×10^{-1} M, respectively, at 40°C for 30 seconds. An excess solution in the TiO_2/MgO films was washed with ethanol and calcined at 450°C for 30 minutes. Then, the TiO_2/MgO composite films were immersed in the 0.1 M $AgNO_3$ solution for 5 seconds, then rinsed with DI water, and dried in a N_2 stream. The films were then exposed to UV irradiation at λ = 254 nm using a Spectroline CM-10 Fluorescence Analysis Cabinet at an intensity of ~0.31 mW/cm^2. We designed the experiment to vary exposure times for 5, 120, and 240 minutes for the photocatalytic reduction of Ag^+ to the metallic Ag nanoparticles [4], to form the Ag nanoparticles size of approximately 4.4, 19.2, and 38.6 nm, respectively. Finally, the TiO_2/MgO/Ag composite electrodes were immersed in dye solution for 48 hours at room temperature and prepared as working electrodes of the DSSCs.

2.3. The Preparation of Pt Counter Electrodes. The counter electrodes were prepared by screen printing a thin layer of platinum (Pt) with a size of $0.5 \times 1.2\,cm^2$ using a platinum paste (Dyesol), on a FTO glass substrate ($2 \times 3\,cm^2$), and then sintered at 450°C for 30 minutes.

2.4. DSC Fabrication. A sandwich-type cell [21] was fabricated by assembling a sensitized TiO_2 electrode using Surlyn-based polymer sheet (80 μm thick) and sealed by a hot gun for a few seconds. The liquid electrolyte contained 0.5 M LiI, 0.05 M I_2, and 0.5 M 4-*tert*-butylpyridine in 90 : 10 v/v of acetonitrile : 3-methyl-2-oxazolidinone. Electrolyte injecting holes, made on the counter-electrode side, were sealed with Surlyn and glass cover.

2.5. Measurements. Optical absorption spectra of the film electrode samples were measured using a UV-Visible Spectrophotometer (Jasco model: V-530). In order to observe the microstructure and elemental analysis of the obtained Ag nanoparticles, the Ag nanoparticles were prepared on carbon-coated copper grids for observations by transmission electron microscopy (TEM JEOL model: JSM-2010). The X-ray diffraction (XRD JEOL- 300) patterns were obtained by analyzing the Ag/TiO_2 films on the glass substrates. Scanning electron microscope (SEM JEOL model: JSM-6301F with attached energy dispersive X-Ray Spectrometer (EDX)) was employed to record cross-sectional micrographs of the Ag/TiO_2 films. *J-V* measurements were performed under a 450 W xenon light source which is able to provide 1000 W·m^{-2} sunlight equivalent irradiation (AM 1.5), using Keithley digital source meter (model 2400) under the illuminated condition.

3. Results and Discussion

3.1. The Morphology of the TiO_2/MgO/Ag Composite Films. Figures 1–3 show appearances of the TiO_2/Ag, TiO_2/MgO, and TiO_2/MgO/Ag composite films, respectively.

Results show that the TiO_2/Ag composite films are brown and become darker with the longer UV exposure time due to a prolonged photocatalytic reduction of Ag^+ to Ag [22], while the TiO_2/MgO composite films are white and translucent. Therefore, the colors of the TiO_2/MgO/Ag composite films come from the Ag nanoparticles.

Figures 4(a), 4(b), and 4(c) show surface images of bare-TiO_2, TiO_2/MgO (0.10 nm)/Ag (4.4 nm), and TiO_2/MgO (0.46 nm)/Ag (4.4 nm) composited films by SEM, respectively. The MgO thin film and Ag nanoparticles cannot be observed because of their ultrathin and ultrasmall nature [6, 23]. Figure 4(d) shows cross section image of the TiO_2/MgO (0.10 nm)/Ag (4.4 nm) composite film showing the film thickness of approximately 11.15 μm.

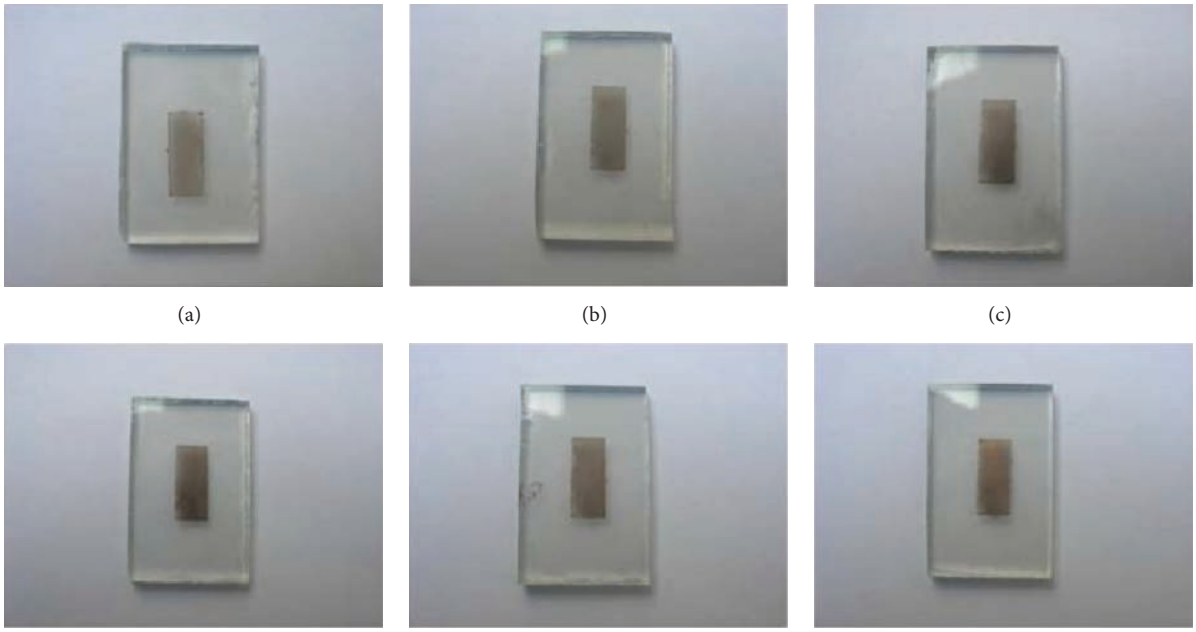

FIGURE 1: The TiO_2/Ag composite films with varied UV exposure time as 5, 30, 60, 120, 180, and 240 min, corresponding to the silver nanoparticle sizes of (a) 4.4 nm, (b) 7.2 nm, (c) 11 nm, (d) 19.2 nm, (e) 27.5 nm, and (f) 38.6 nm, respectively [4, 5].

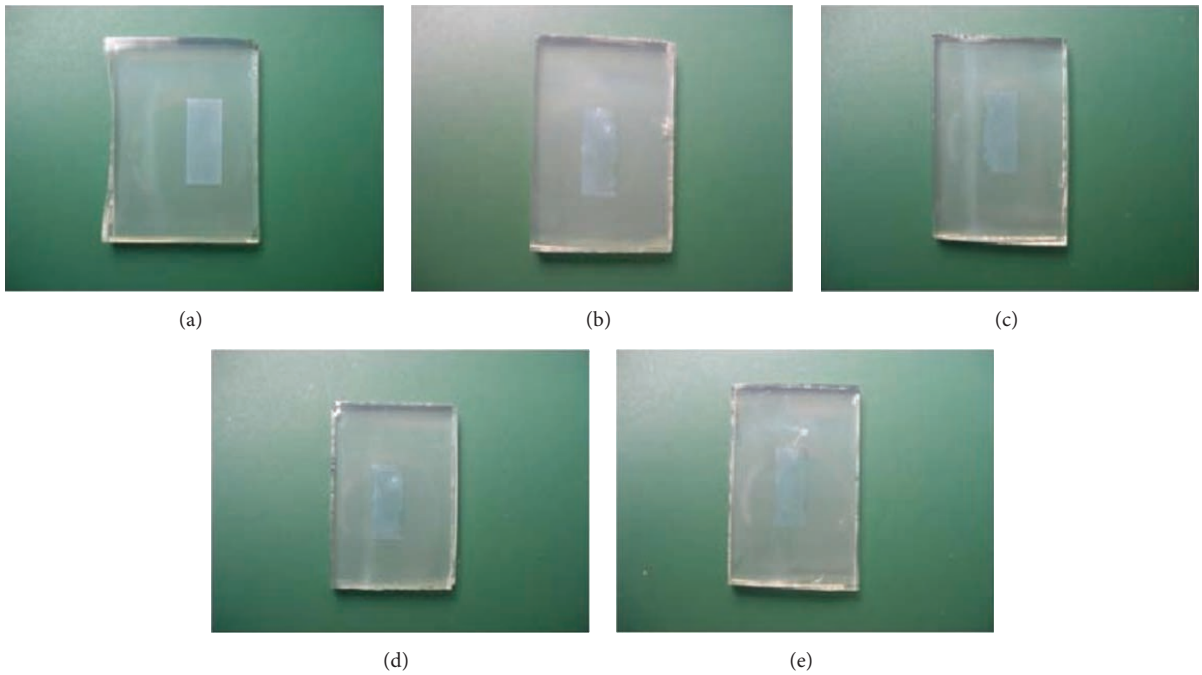

FIGURE 2: The TiO_2/MgO composite films with varied magnesium acetate solution concentrations of 1×10^{-4} M, 1×10^{-3} M, 1×10^{-2} M, and 1×10^{-1} M. These correspond to the MgO film thicknesses of (a) bare-TiO_2, (b) 0.08 nm, (c) 0.10 nm, (d) 0.16 nm, and (e) 0.46 nm, respectively [6].

The EDX technique of SEM was used to analyze the elements of Ti, Mg, and Ag, resulting in the peaks of Ti and Ag that were found on the surface image of the TiO_2/MgO (0.10 nm)/Ag (4.4 nm) composite film but the Mg peak was not found suggesting that it was rinsed off from the film surface as shown in Figure 5(a). However, Mg peak was present in the cross section of the TiO_2/MgO (0.10 nm) Ag (4.4 nm) composite film (see Figure 4(d)) indicating the presence of Mg element as shown in Figure 5(b).

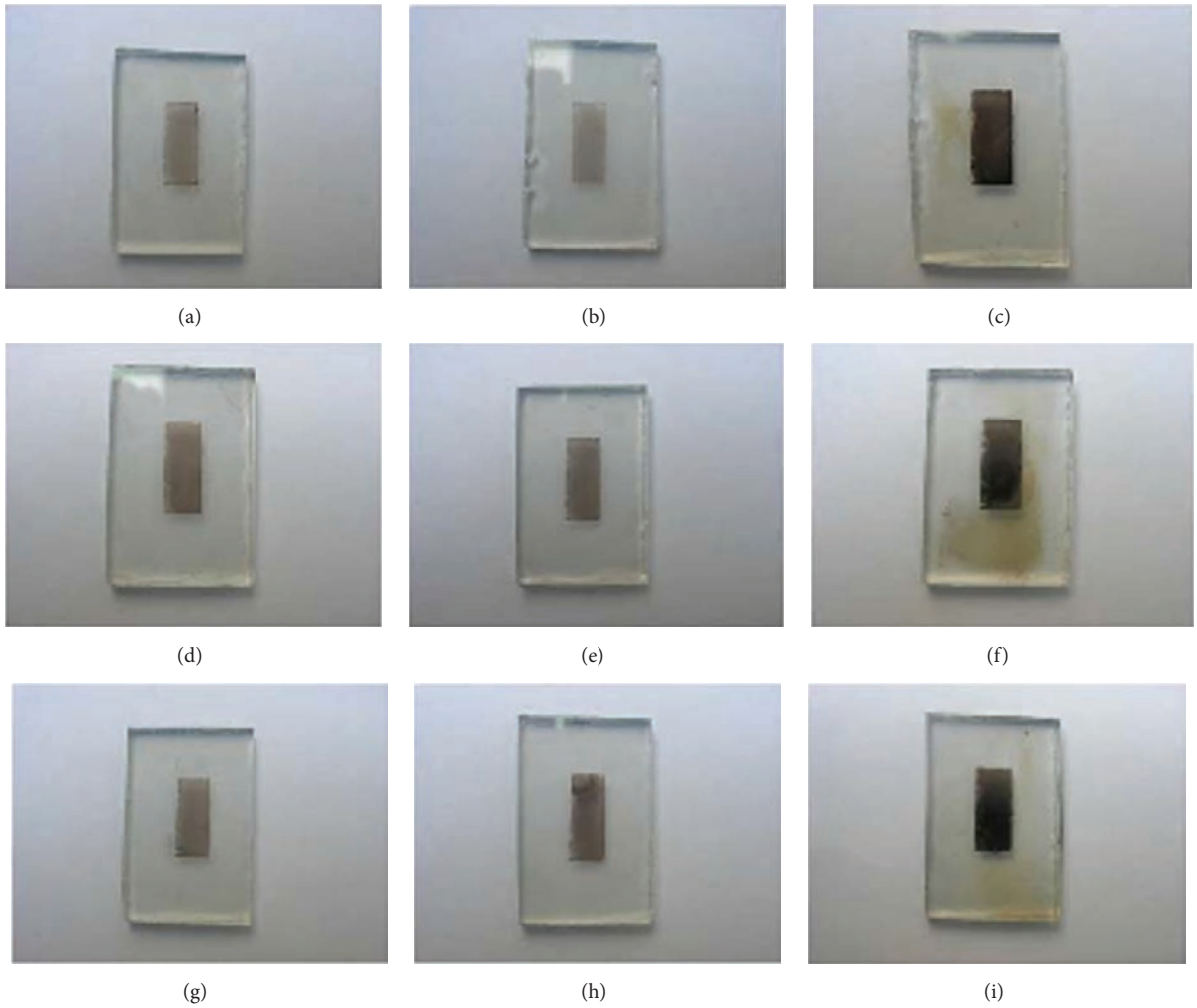

Figure 3: The TiO_2/MgO/Ag composite films with varied magnesium acetate solution concentrations and silver nanoparticles sizes: (a) TiO_2/MgO (0.08 nm)/Ag (4.4 nm), (b) TiO_2/MgO (0.10 nm)/Ag (4.4 nm), (c) TiO_2/MgO (0.46 nm)/Ag (4.4 nm), (d) TiO_2/MgO (0.08 nm)/Ag (19.2 nm), (e) TiO_2/MgO (0.10 nm)/Ag (19.2 nm), (f) TiO_2/MgO (0.46 nm)/Ag (19.2 nm), (g) TiO_2/MgO (0.08 nm)/Ag (38.6 nm), (h) TiO_2/MgO (0.10 nm)/Ag (38.6 nm), and (i) TiO_2/MgO (0.46 nm)/Ag (38.6 nm).

Figure 6 shows a TEM image of the TiO_2/MgO (0.10 nm) composite film. However, we can not observe the magnesium oxide thin film on surfaces of the TiO_2 nanoparticles because of its ultrathin nature. The MgO content of the film was estimated by the extraction of MgO with HCl and atomic adsorption spectrophotometric estimation. The thickness t of the MgO film was calculated as t = (weight of MgO)/$S\rho$, where S = surface area of TiO_2 (S determined by the desorption of the dye into an alcoholic alkaline solution and spectrophotometric estimation = 560 times geometrical cross section of the film = 1 cm^2) and ρ = density of MgO [23]. The concentrations of magnesium acetate solution of 1×10^{-4}, 1×10^{-3}, and 1×10^{-1} M were calculated to give the thicknesses of the magnesium oxide film as 0.08, 0.10, and 0.46 nm, respectively.

3.2. The Effect of the MgO Thin Film and Ag Nanoparticle Size on Optical Absorption Spectra. Figure 7 shows a comparison of the optical absorption spectra in the range of 370–800 nm between the bare-TiO_2, TiO_2/Ag, TiO_2/MgO, and TiO_2/MgO/Ag composite films. The optical absorption spectra of the bare-TiO_2 film and TiO_2/MgO composite film were found to be similar and lower than those of the TiO_2/Ag (19.20 nm) and TiO_2/MgO (0.10 nm)/Ag (4.40 nm) composite films. This agrees with research results of Bandara et al., reporting that a coating of MgO on TiO_2 does not change the absorption property of TiO_2 as MgO electron excitation energy falls above the excitation energy of TiO_2 [21].

However, for the cases of TiO_2/Ag (19.20 nm) and TiO_2/MgO (0.10 nm)/Ag (4.40 nm) composite films, the optical absorption spectra have much higher absorption than the previous two cases at a wavelength range of around 400–600 nm. The optical absorption of the TiO_2/MgO (0.10 nm)/Ag (4.40 nm) composite film is slightly higher than the TiO_2/Ag (19.20 nm) film in the wavelength range

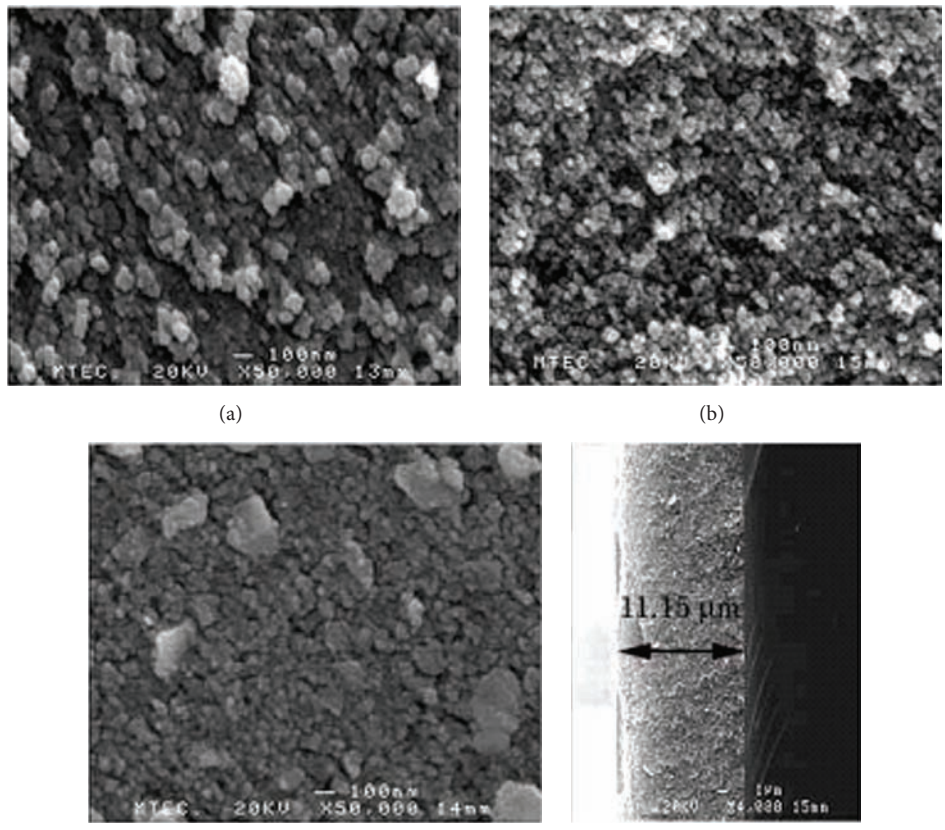

Figure 4: SEM images of TiO_2/MgO/Ag composite films: (a) bare-TiO_2, (b) TiO_2/MgO (0.10 nm)/Ag (4.4 nm), (c) TiO_2/MgO (0.46 nm)/Ag (4.4 nm), and (d) cross section of TiO_2/MgO (0.10 nm)/Ag (4.4 nm).

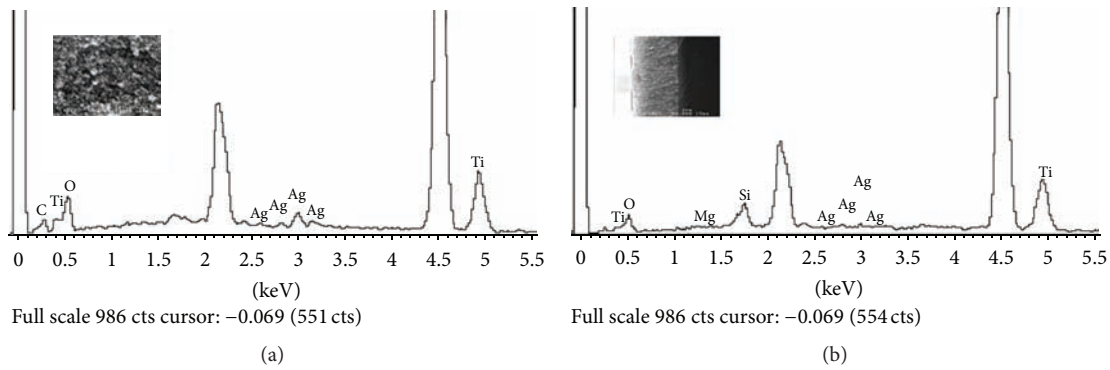

Figure 5: EDX spectra taken from (a) surface and (b) cross section of TiO_2/MgO (0.10 nm)/Ag (4.4 nm) composite film.

of 400–600 nm, whereas in the wavelength range of 600–800 nm we found that the optical absorption spectrum of the TiO_2/Ag (19.2 nm) composite film is higher than that of the TiO_2/MgO (0.10 nm)/Ag (4.40 nm) composite film. Therefore, the Ag nanoparticles have been shown clearly to improve optical adsorption due to plasmon energy transfer effect [4, 9, 12, 13]. In addition, the light scattering effect of Ag nanoparticles enhances the absorption of photoanode [24].

When we consider the optical absorption spectrum of TiO_2/MgO/Ag with the fixed MgO film thickness of 0.10 nm and varied Ag nanoparticles size in a range of 4.40–38.60 nm, the optical absorption of the bare-TiO_2 has the lowest value, while the optical absorption of TiO_2/MgO (0.10 nm)/Ag (38.60 nm) has the highest value as shown in Figure 8. The red shifted nature of the spectrum indicates surface plasmon effect [4, 25].

Although, for the 0.1 nm thick MgO thin films, the Ag nanoparticles are more influential than the MgO thin film

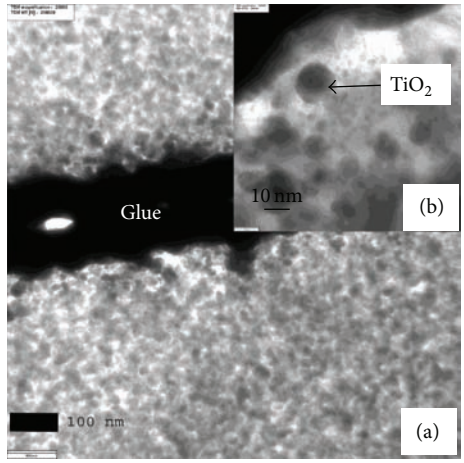

Figure 6: A cross-sectional TEM micrograph of the TiO_2/MgO (0.10 nm) composite films prepared from 1×10^{-3} M of magnesium acetate solution (a) ×20,000, (b) ×200,000.

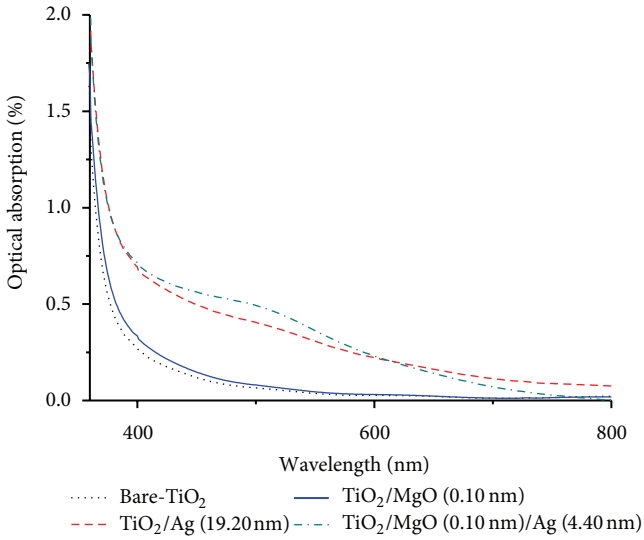

Figure 7: Optical absorption spectra of the bare-TiO_2 film compared with the TiO_2/Ag (19.2 nm), TiO_2/MgO (0.10 nm), and TiO_2/MgO/Ag composite films.

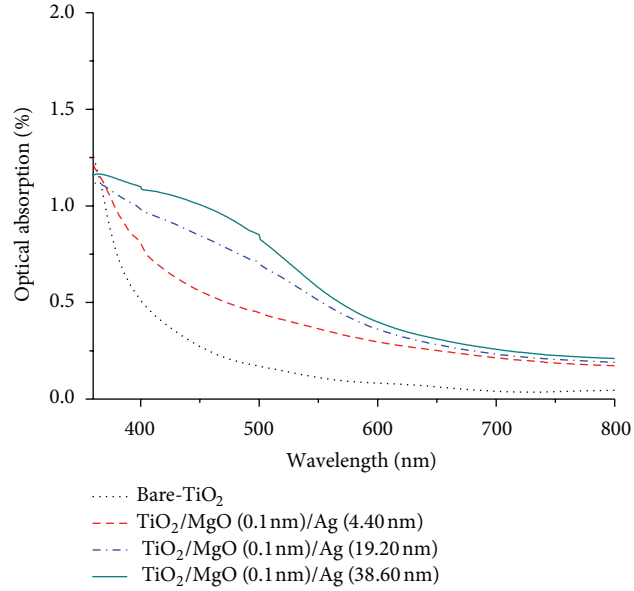

Figure 8: Optical absorption spectra of the bare-TiO_2 compared with the TiO_2/MgO/Ag composite films with varied Ag nanoparticle size in range of 4.40–38.60 nm.

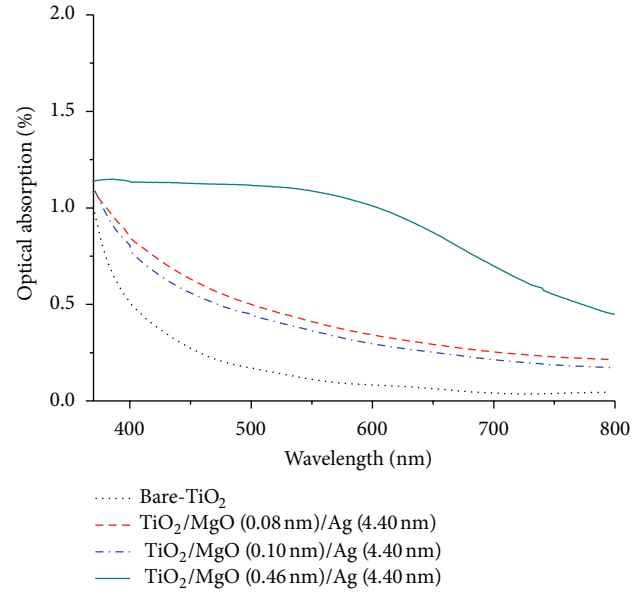

Figure 9: Optical absorption spectra of the TiO_2/MgO/Ag composite films with varied film thicknesses of magnesium oxide in range of 0.08–0.46 nm.

on the TiO_2 film for optical absorption (Figure 7), the optical absorption can be increased with increasing thickness of the MgO thin film as shown in Figure 9.

3.3. The Effect of the MgO Ultrathin Film and Ag Nanoparticles on Efficiency of the DSSCs. The efficiency of DSSCs with TiO_2/MgO (0.10 nm)/Ag (4.40 nm) composite electrode has the highest efficiency among all conditions prepared including the bare-TiO_2 electrode as shown in Table 1.

The results showed that the maximum efficiency of the DSSCs was obtained with TiO_2/MgO (0.10 nm)/Ag (4.4 nm) composite electrode (Figure 10). The DSSCs with TiO_2/MgO (0.10 nm)/Ag (4.4 nm) have the maximum efficiency, although this condition did not give the highest optical absorption (see Figure 9). The maximum efficiency obtained suggests that the MgO layer coated on the TiO_2 film acts as a recombination barrier at the TiO_2/MgO/Ag contacts and becomes a dominant effect [9, 11, 26, 27].

In addition, the efficiency of the DSSCs depends on the MgO film thickness, the maximum efficiency of DSSCs with TiO_2/MgO (0.10 nm)/Ag (4.4 nm) working electrode. When the MgO film thickness increased, the efficiency of DSSCs is decreased, as shown in Figure 11.

Table 1: Optimization of the TiO_2/MgO/Ag composite films by varying the MgO thin film thickness and the Ag nanoparticles size for enhanced efficiency of the DSSCs.

Silver nanoparticles size (nm)	Efficiency of DSSCs (%) Magnesium oxide film thickness (nm)			Efficiency of bare-TiO_2 DSSCs (%)
	0.08	0.10	0.46	
4.40	5.1 ± 0.1	5.2 ± 0.1	2.6 ± 0.2	3.8 ± 0.1
19.20	4.1 ± 0.2	4.1 ± 0.1	2.0 ± 0.3	
38.60	3.7 ± 0.1	3.8 ± 0.2	1.1 ± 0.6	

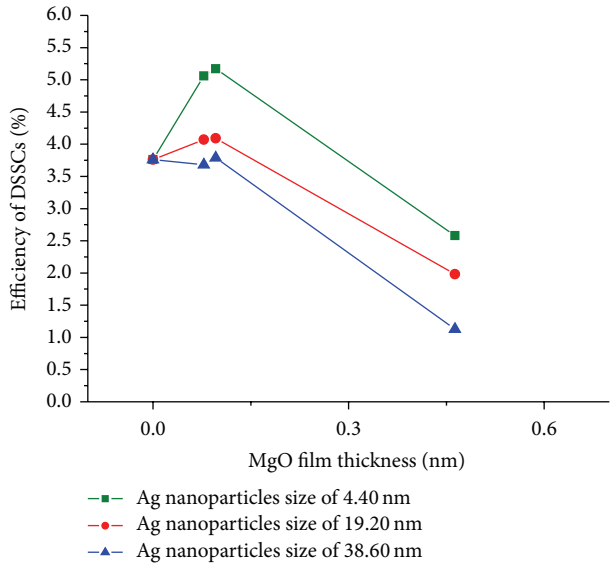

Figure 10: The efficiency of DSSCs with the bare-TiO_2 film and the TiO_2/MgO (0.10 nm)/Ag composite films with various Ag nanoparticles sizes in range of 4.40–38.60 nm.

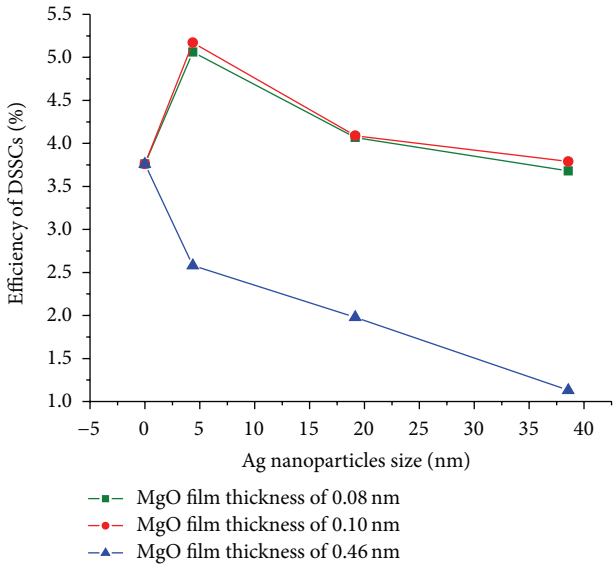

Figure 11: The efficiency of DSSCs with the bare-TiO_2 film and the TiO_2/MgO/Ag composite films with various MgO film thicknesses in range of 0.08–0.46 nm.

Using the same materials and structure and improving the TiO_2 working electrode by coating the Ag nanoparticles alone on the TiO_2 film for increase in light absorption coefficient of the dye molecule, the efficiency up to 4.8% was obtained [4]. The coating of the MgO thin films on the TiO_2 films to reduce the recombination process between the electron on conduction band of TiO_2 and triiodide in the electrolyte was reported to increase the efficiency up to 5.0% [6]. While the conventional DSSCs fabricated have efficiency about 3.8%, both methods can improve the efficiency of DSSCs and lead to the coating TiO_2 working electrode by MgO thin film and Ag nanoparticles for a novel TiO_2/MgO/Ag working electrode in this study. The DSSCs using the TiO_2/MgO (0.10 nm)/Ag (4.40 nm) composite film as working electrode have the maximum efficiency of approximately 5.2%, when compared with the DSSCs using other working electrodes such as the bare-TiO_2, TiO_2/Ag (19.20 nm) [4], and TiO_2/MgO (0.10 nm) [6] as shown in Figure 12. When the Ag nanoparticles bigger than 4.4 nm were coated on TiO_2/MgO (0.10 nm) composite film, the efficiency decreases, supposedly because the Schottky barriers were formed at the TiO_2/MgO/Ag contacts, became dominant, and retarded electron transport in the conduction bands [9, 11].

Electrochemical impedance spectra (EIS) of the DSSCs can describe the internal resistances of the DSSCs. R_1 is related to the carrier transport resistance at the surface of Pt counter electrode, R_2 is related to carrier transport resistance at the TiO_2/dye/electrolyte interface, and R_3 is related to the diffusion of iodide and triiodide within the electrolyte.

Figure 13 shows EIS results of the DSSCs with the bare-TiO_2 and the TiO_2/MgO/Ag (4.4 nm) electrodes with varied MgO film thicknesses. We found that the EIS of the DSSCs with the TiO_2/MgO (0.10 nm)/Ag (4.4 nm) composite electrode have the smallest curve of R_2. Thus the carrier transport resistance in TiO_2/dye/electrolyte interface is the lowest at the MgO film thickness of 0.10 nm, which is consistent with the shunt resistance (R_{SH}) of the DSSCs with the TiO_2/MgO (0.10 nm)/Ag (4.40 nm) composite electrode with lowest value of 2.70 kΩ $*$ cm^2 (see Table 2). This is due to the high value of R_{SH} indicating a slow back electron transfer rate from the TiO_2 to the electrolytes at the TiO_2/dye/electrolyte interface [28]. Increasing the MgO film thickness to exceed 0.10 nm, I_{SC} decreases because electron injection from the excited dye molecules to the CB of TiO_2 is hindered by the MgO film. An optimum of the MgO film thickness acts as the energy barrier to hinder the recombination process [6, 8]. However, as the MgO film thickness increases, V_{OC}

Table 2: The short circuit current densities (I_{SC}), open circuit voltages (V_{OC}), fill factors (FF), efficiencies, series resistances (R_S), and shunt resistances (R_{SH}) of DSSCs prepared using the TiO_2/MgO/Ag composite film electrodes compared with bare-TiO_2 electrode (reference) under AM1.5.

Condition of working electrodes	I_{SC} (mA)	V_{OC} (V)	FF	Efficiency (%)	R_S ($\Omega*cm^2$)	R_{SH} ($k\Omega*cm^2$)
Bare-TiO_2	6.60	0.71	0.81	3.80	10.02	2.87
TiO_2/MgO (0.08 nm)/Ag (4.4 nm)	8.37	0.78	0.74	5.10	10.39	2.69
TiO_2/MgO (0.10 nm)/Ag (4.4 nm)	8.63	0.79	0.76	5.20	15.14	2.70
TiO_2/MgO (0.46 nm)/Ag (4.4 nm)	4.42	0.80	0.72	2.60	36.38	4.97
TiO_2/MgO (0.08 nm)/Ag (19.2 nm)	6.70	0.77	0.79	4.10	15.39	3.70
TiO_2/MgO (0.10 nm)/Ag (19.2 nm)	6.94	0.78	0.75	4.10	18.67	4.35
TiO_2/MgO (0.46 nm)/Ag (19.2 nm)	3.46	0.79	0.72	2.0	41.63	4.62
TiO_2/MgO (0.08 nm)/Ag (38.6 nm)	6.25	0.76	0.78	3.70	15.75	4.35
TiO_2/MgO (0.10 nm)/Ag (38.6 nm)	6.29	0.77	0.78	3.80	20.40	3.92
TiO_2/MgO (0.46 nm)/Ag (38.6 nm)	2.00	0.79	0.68	1.10	61.87	6.22

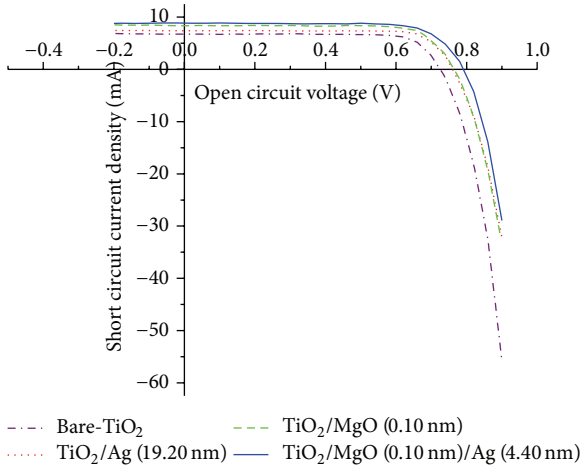

Figure 12: Comparison of the efficiencies of DSSCs with different types of electrodes, that is, the bare-TiO_2, TiO_2/Ag (19.2 nm), TiO_2/MgO (0.10 nm), and TiO_2/MgO (0.10 nm)/Ag (4.4 nm) electrodes.

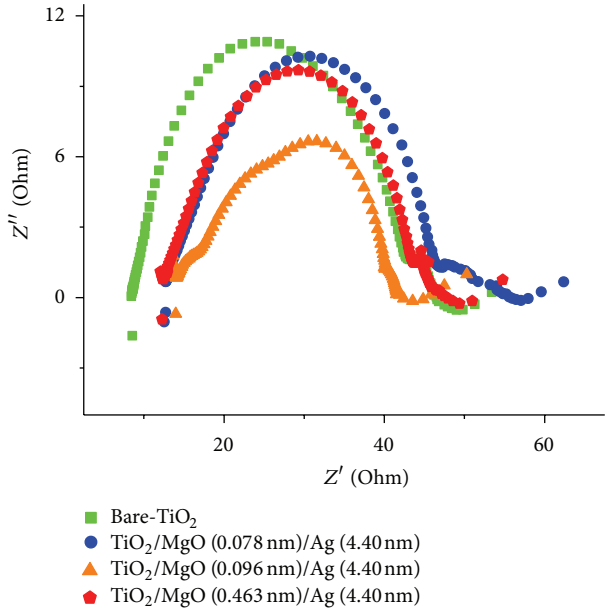

Figure 13: Electrochemical impedance spectra (EIS) of DSSCs with the TiO_2/MgO/Ag (4.4 nm) electrodes with varied thickness of MgO.

will increase accordingly (Table 2) due to a negative shift of flat band potential after coating the thin MgO layer on the semiconductor particles. V_{OC} is determined by the difference between the quasi-Fermi level of electron in the oxide film and the energy of the redox couple in the electrolyte [29].

Electrochemical impedance spectra (EIS) of the DSSCs with varying Ag nanoparticle size ranging from 4.40 to 38.6 nm in the TiO_2/MgO (0.10 nm)/Ag composite electrodes are shown in Figure 14. The EIS of DSSCs with the TiO_2/MgO (0.10 nm)/Ag (4.40 nm) composite electrode were found to have the smallest curve, indicating that the carrier transport resistance at the TiO_2/dye/electrolyte interface is the lowest. When the Ag nanoparticle size increases more than 4.4 nm, the carrier transport resistance in TiO_2/dye/electrolyte interface was found to increase because of the Schottky barriers formed at the TiO_2/MgO/Ag contacts [9, 11].

4. Conclusion

The TiO_2/MgO/Ag composite electrode was prepared with the MgO thin film and the Ag nanoparticles by dipping and photoreduction method, respectively. The efficiency enhancement of the DSSCs is based on the principle of ultrathin outer shell of insulator and surface plasmon resonance. The optimum condition obtained was TiO_2/MgO/Ag composite film consisting of the MgO film thickness of 0.10 nm and Ag nanoparticles size of 4.40 nm to give a maximum efficiency of 5.2%. The EIS of the DSSCs with the TiO_2/MgO (0.10 nm)/Ag (4.4 nm) composite electrode showed the lowest carrier transport resistance at the TiO_2/dye/electrolyte interface. The Ag nanoparticles influenced the optical absorption of the TiO_2 film because of the surface plasmon resonance induced by the silver nanoparticles enhancing Raman

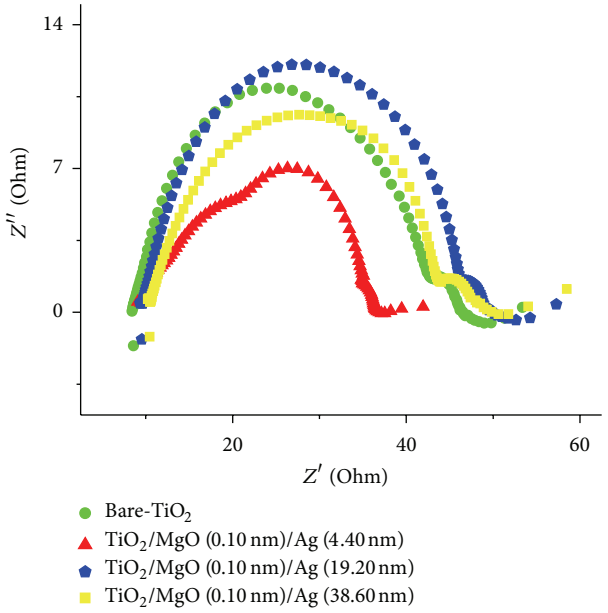

FIGURE 14: Electrochemical impedance spectra (EIS) of DSSCs with the TiO_2/MgO (0.10 nm)/Ag electrodes with varied Ag nanoparticles size.

scattering and optical absorption of the dye. A coating of MgO on the TiO_2 acted as the energy barrier to hinder the recombination process and was found to significantly improve cell efficiency.

Conflict of Interests

The authors declare that there is no conflict of interests regarding the publication of this paper.

Acknowledgments

The authors thank the National Metal and Materials Technology Center (MTEC) and Suan Dusit University, Thailand, for financial support.

References

[1] B. O'Regan and M. Grätzel, "A low-cost, high-efficiency solar cell based on dye-sensitized colloidal TiO_2 films," *Nature*, vol. 353, no. 6346, pp. 737–740, 1991.

[2] D. S. Tsoukleris, I. M. Arabatzis, E. Chatzivasiloglou et al., "2-Ethyl-1-hexanol based screen-printed titania thin films for dye-sensitized solar cells," *Solar Energy*, vol. 79, no. 4, pp. 422–430, 2005.

[3] C. O. Avellaneda, A. D. Gonçalves, J. E. Benedetti, and A. F. Nogueira, "Preparation and characterization of core-shell electrodes for application in gel electrolyte-based dye-sensitized solar cells," *Electrochimica Acta*, vol. 55, no. 4, pp. 1468–1474, 2010.

[4] C. Photiphitak, P. Rakkwamsuk, P. Muthitamongkol, C. Sae-Kung, and C. Thanachayanont, "Effect of silver nanoparticle size on efficiency enhancement of dye-sensitized solar cells," *International Journal of Photoenergy*, vol. 2011, Article ID 258635, 8 pages, 2011.

[5] C. Photiphitak, P. Rakkwamsuk, P. Muthitamongkol, C. Sae-Kung, and C. Thanachayanont, "Effect of silver nanoparticles size prepared by photoreduction method on optical absorption spectra of TiO_2/Ag/N719 dye composite films," in *Proceedings of the International Conference on Chemical and Biological Engineering*, pp. 6–9, December 2010.

[6] C. Photiphitak, P. Rakkwamsuk, P. Muthiamongkol, and C. Thanachayanont, "Performance enhancement of dye-sensitized solar cells by MgO coating on TiO_2 electrodes," in *Proceedings of the International Conference on Electrical, Computer, Electronics and Communication Engineering*, pp. 485–489, Bangkok, Thailand, March 2012.

[7] Z. Liu, K. Pan, M. Liu et al., "Al_2O_3-coated SnO_2/TiO_2 composite electrode for the dye-sensitized solar cell," *Electrochimica Acta*, vol. 50, no. 13, pp. 2583–2589, 2005.

[8] J. Bandara, S. S. Kuruppu, and U. W. Pradeep, "The promoting effect of MgO layer in sensitized photodegradation of colorants on TiO_2/MgO composite oxide," *Colloids and Surfaces A: Physicochemical and Engineering Aspects*, vol. 276, no. 1–3, pp. 197–202, 2006.

[9] C. Wen, K. Ishikawa, M. Kishima, and K. Yamada, "Effects of silver particles on the photovoltaic properties of dye-sensitized TiO_2 thin films," *Solar Energy Materials and Solar Cells*, vol. 61, no. 4, pp. 339–351, 2000.

[10] K.-C. Lee, S.-J. Lin, C.-H. Lin, C.-S. Tsai, and Y.-J. Lu, "Size effect of Ag nanoparticles on surface plasmon resonance," *Surface and Coatings Technology*, vol. 202, no. 22-23, pp. 5339–5342, 2008.

[11] G. Zhao, H. Kozuka, and T. Yoko, "Effects of the incorporation of silver and gold nanoparticles on the photoanodic properties of rose bengal sensitized TiO_2 film electrodes prepared by sol-gel method," *Solar Energy Materials and Solar Cells*, vol. 46, no. 3, pp. 219–231, 1997.

[12] A. M. Glass, P. F. Liao, J. G. Bergman, and D. H. Olson, "Interaction of metal particles with adsorbed dye molecules: absorption and luminescence," *Optics Letters*, vol. 5, no. 9, pp. 368–370, 1980.

[13] Z. Y. Zhu, C. Mao, R. Y. Yang, L. X. Dai, and C. S. Nie, "Surface-enhanced Raman scattering of Ru(II) homo- and heterolytic complexes with 2,2′-bipyridine and 1,1′-biisoquinoline in aqueous silver sol," *Journal of Raman Spectroscopy*, vol. 24, no. 4, pp. 221–226, 1993.

[14] W.-J. Yoon, K.-Y. Jung, J. Liu et al., "Plasmon-enhanced optical absorption and photocurrent in organic bulk heterojunction photovoltaic devices using self-assembled layer of silver nanoparticles," *Solar Energy Materials and Solar Cells*, vol. 94, no. 2, pp. 128–132, 2010.

[15] D. M. Schaadt, B. Feng, and E. T. Yu, "Enhanced semiconductor optical absorption via surface plasmon excitation in metal nanoparticles," *Applied Physics Letters*, vol. 86, no. 6, Article ID 063106, 2005.

[16] C. F. Eagen, "Nature of the enhanced optical absorption of dye-coated Ag island films," *Applied Optics*, vol. 20, no. 17, pp. 3035–3042, 1981.

[17] J. J. Mock, M. Barbic, D. R. Smith, D. A. Schultz, and S. Schultz, "Shape effects in plasmon resonance of individual colloidal silver nanoparticles," *The Journal of Chemical Physics*, vol. 116, no. 15, pp. 6755–6759, 2002.

[18] P. Royer, J. P. Goudonnet, R. J. Warmack, and T. L. Ferrell, "Substrate effects on surface-plasmon spectra in metal-island films," *Physical Review B*, vol. 35, no. 8, pp. 3753–3759, 1987.

[19] G. Xu, M. Tazawa, P. Jin, S. Nakao, and K. Yoshimura, "Wavelength tuning of surface plasmon resonance using dielectric layers on silver island films," *Applied Physics Letters*, vol. 82, no. 22, pp. 3811–3813, 2003.

[20] M. Ihara, K. Tanaka, K. Sakaki, I. Honma, and K. Yamada, "Enhancement of the absorption coefficient of cis-(NCS)2 Bis(2, 2′-bipyridyl-4, 4′-dicarboxylate) ruthenium (II) dye-sentisized solar cells by a silver island film," *Journal of Physical Chemistry B*, vol. 101, pp. 153–157, 1997.

[21] J. Bandara, C. C. Hadapangoda, and W. G. Jayasekera, "TiO_2/MgO composite photocatalyst: the role of MgO in photoinduced charge carrier separation," *Applied Catalysis B: Environmental*, vol. 50, no. 2, pp. 83–88, 2004.

[22] Y. Ohko, T. Tatsuma, T. Fujii et al., "Multicolour photochromism of TiO_2 films loaded with silver nanoparticles," *Nature Materials*, vol. 2, no. 1, pp. 29–31, 2003.

[23] G. R. A. Kumara, M. Okuya, K. Murakami, S. Kaneko, V. V. Jayaweera, and K. Tennakone, "Dye-sensitized solid-state solar cells made from magnesiumoxide-coated nanocrystalline titanium dioxide films: enhancement of the efficiency," *Journal of Photochemistry and Photobiology A: Chemistry*, vol. 164, no. 1–3, pp. 183–185, 2004.

[24] H. Dong, Z. Wu, Y. Gao et al., "Silver-loaded anatase nanotubes dispersed plasmonic composite photoanode for dye-sensitized solar cells," *Organic Electronics*, vol. 15, no. 11, pp. 2847–2854, 2014.

[25] K. Guo, M. Li, X. Fang et al., "Preparation and enhanced properties of dye-sensitized solar cells by surface plasmon resonance of Ag nanoparticles in nanocomposite photoanode," *Journal of Power Sources*, vol. 230, pp. 155–160, 2013.

[26] N. K. Swami, S. Srivastava, and H. M. Ghule, "The role of the interfacial layer in Schottky barrier solar cells," *Journal of Physics D: Applied Physics*, vol. 12, article 765, 1979.

[27] C. M. H. Klimpke and P. T. Landsberg, "An improved analysis of the schottky barrier solar cell," *Solid State Electronics*, vol. 24, no. 5, pp. 401–406, 1981.

[28] L. Han, N. Koide, Y. Chiba, A. Islam, and T. Mitate, "Modeling of an equivalent circuit for dye-sensitized solar cells: improvement of efficiency of dye-sensitized solar cells by reducing internal resistance," *Comptes Rendus Chimie*, vol. 9, no. 5-6, pp. 645–651, 2006.

[29] J. Bandara and U. W. Pradeep, "Tuning of the flat-band potentials of nanocrystalline TiO_2 and SnO_2 particles with an outer-shell MgO layer," *Thin Solid Films*, vol. 517, no. 2, pp. 952–956, 2008.